

# Closing the atmospheric energy budget: Investigation of the residual in column integrated atmospheric energy balance using cloud objects

Seiji Kato<sup>1</sup>, Kuan-Man Xu<sup>1</sup>, Takmeng Wong<sup>1</sup>, Norman G. Loeb<sup>1</sup>,  
Fred G. Rose<sup>2</sup>,  
Kevin E. Trenberth<sup>3</sup>, and Tyler J. Thorsen<sup>4</sup>

<sup>1</sup>NASA Langley Research Center

<sup>2</sup>Science System & Applications Inc.

<sup>3</sup>National Center for Atmospheric Research

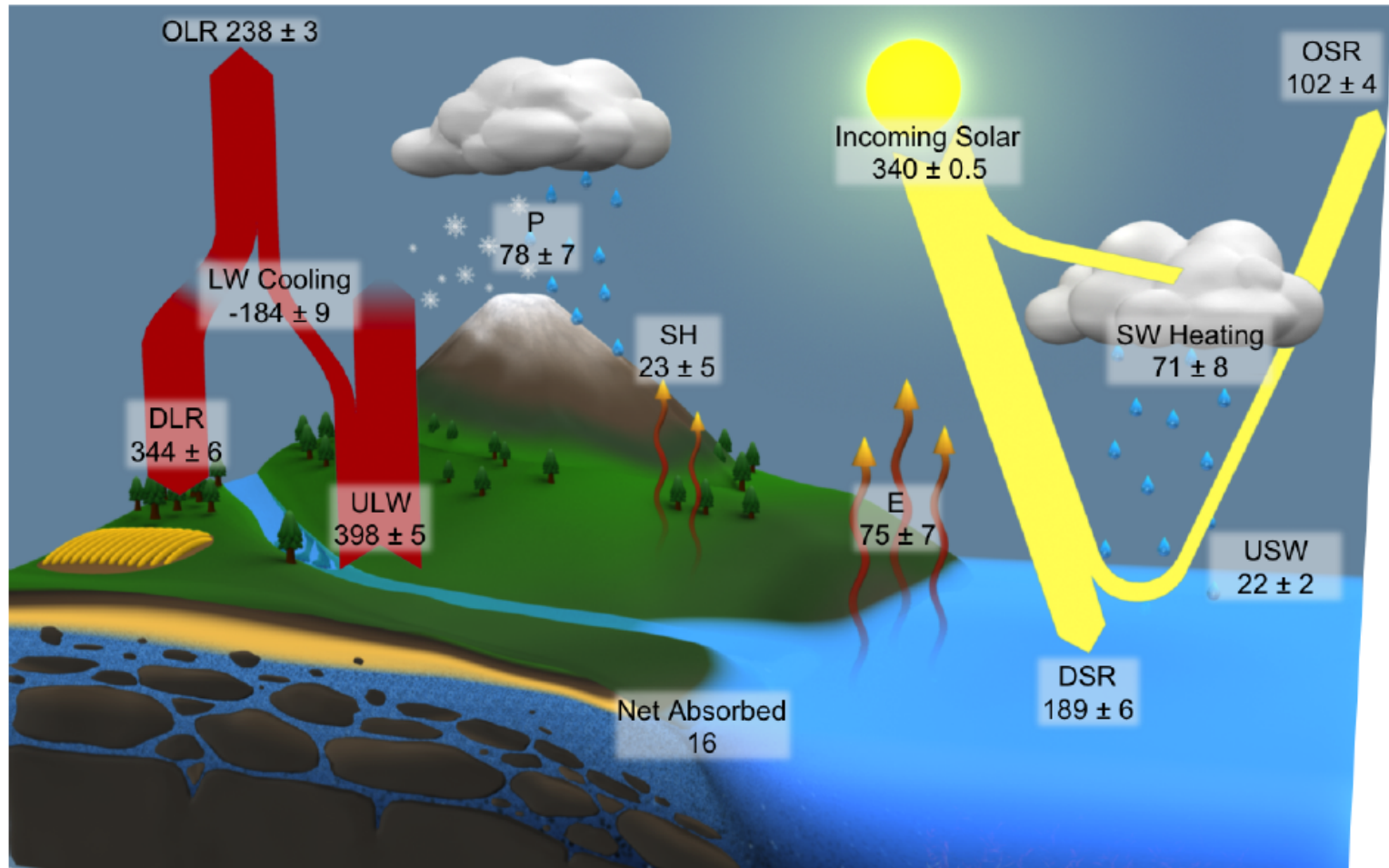
<sup>4</sup>NASA Postdoctoral program



# Outline

- Current status of satellite derived surface energy budget
- Radiation budget
  - Uncertainty and evaluation of computed irradiance with surface observations
- Atmospheric energy budget
- Regions with large energy residual
- Cloud type associated with large energy residual

# Current status of satellite based surface energy balance residual in $\text{Wm}^{-2}$



L'Ecuyer et al. 2015 (J. Climate)

Surface:  $344 - 398 - 23 - 75 + 189 - 22 = 15 \text{ Wm}^{-2}$  (depending on data sets used)

Ocean heating rate:  $0.53$  to  $0.75 \text{ Wm}^{-2}$  (Lyman et al. 2010 Nature)

$0.4 - 0.6 \text{ Wm}^{-2}$  in  $0$  to  $2000 \text{ m}$  layer (Roemmich et al. 2015)

$0.64 \pm 0.44 \text{ Wm}^{-2}$  for the entire column (Llovel et al. 2014)

# Surface radiation measurement uncertainty

# Surface measurement uncertainty (SW)

Reference	Uncertainty /difference	
Ohmura et al. (1998)	5 Wm <sup>-2</sup> (1 min average)	BSRN accuracy requirement, standard deviation of calibration coefficients
Michalsky et al. (1999)	10 Wm <sup>-2</sup> at solar noon	Component sum method difference of 4 independent measurements
Michalsky et al. (2003)	4 Wm <sup>-2</sup> (diffuse 95% confidence level)	8 diffuse measurements comparison (with thermal offset correction)
Michalsky et al. (2006)	1% direct, 2% diffuse (187 Wm <sup>-2</sup> times 0.02 = 3.7 Wm <sup>-2</sup> )	Model observation comparisons
Michalsky et al. (2007)	±2.2%+0.2 Wm <sup>-2</sup> Diffuse horizontal average	4 diffuse measurements
Colbo and Weller (2009)	20Wm <sup>-2</sup> (instant, 1min), 6 Wm <sup>-2</sup> (daily), 5 Wm <sup>-2</sup> (annual)	radiometers deployed on buoys

# Surface measurement uncertainty (LW)

Reference	Uncertainty /difference	
Ohmura et al. (1998)	10 Wm <sup>-2</sup> (1 min average)	BSRN accuracy requirement, standard deviation of calibration coefficients
Philipona et al. (2001)	2 Wm <sup>-2</sup> (nighttime, 260 to 420 Wm <sup>-2</sup> downward longwave)	Measurement vs. measurements and measurements vs. model.
Colbo and Weller (2009)	7.5 Wm <sup>-2</sup> (instant,1 min), 4 Wm <sup>-2</sup> (daily), 4 Wm <sup>-2</sup> (annual)	radiometers deployed on buoys
Marty et al. (2012)	2 Wm <sup>-2</sup> (120 to 240 Wm <sup>-2</sup> downward longwave irradiance)	Measurement vs. measurements and measurements vs. model.
Gröbner et al. (2014)	2 to 6 Wm <sup>-2</sup> (~2%)	Measurements during 2 IOPs and past 4 years

# Regions with a large energy imbalance

Atmospheric energy balance (Trenberth and Stepaniak 2003)

$$-\left[ \frac{\partial(K_E + S_H + \Phi_s + L_E)}{\partial t} - (R_T - R_s) + H_s + LE + \nabla_p \cdot (\mathbf{F}_K + \mathbf{F}_{DE} + \mathbf{F}_{LE}) \right] = 0$$

Water mass balance

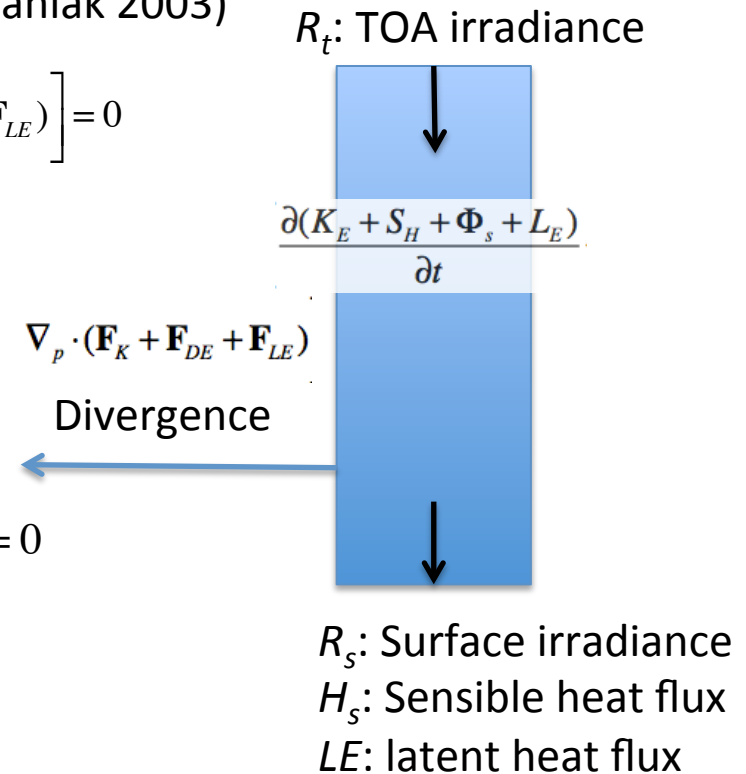
$$-\left[ \frac{\partial L_E}{\partial t} + LP + LE + \nabla_p \cdot \mathbf{F}_{LE} \right] = 0$$

$$-\frac{\partial(K_E + S_H + \Phi_s)}{\partial t} - \nabla_p \cdot (\mathbf{F}_K + \mathbf{F}_{DE}) + (R_T - R_s) + LP - H_s = 0$$

- Kinetic energy + dry static energy tendency
- Kinetic energy divergence
- + atmospheric net irradiance
- + precipitation × (latent heat of vaporization)
- Surface sensible heat flux (positive downward)

Dry static energy = sensible heat flux + potential energy

Neglecting water phase change (the error in the global mean is about 0.8 Wm<sup>-2</sup>)



# Testing atmospheric energy balance using observations

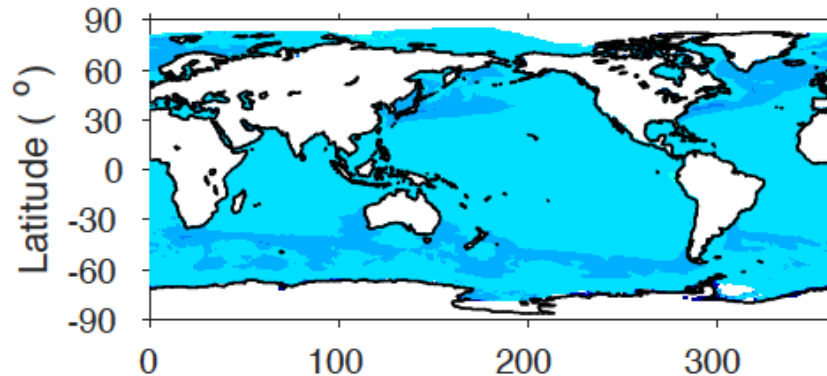
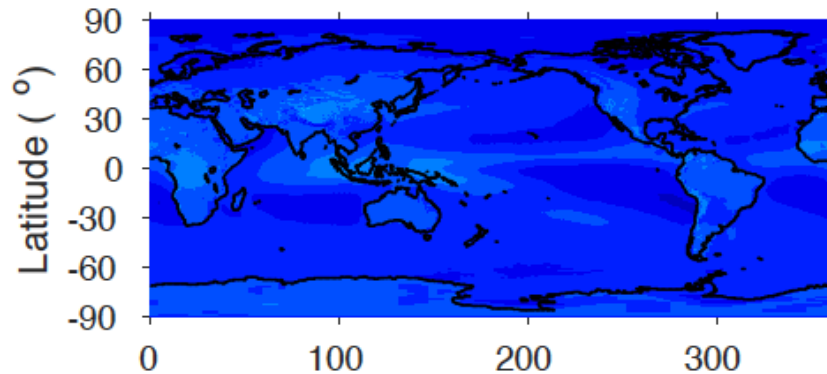
Data source (March 2000 through Feb. 2010)

- Atmospheric net irradiance: EBAF-TOA and EBAF-surface (Ed 2.8, Loeb et al. 2009, 2012; Kato et al. 2013 )
- Precipitation: GPCP (V2.2, Huffman et al. 1997; Adler et al. 2012 )
- Surface sensible and latent heat flux: SeaFlux (Jan 2000 through Dec. 2007, Clayson and Bogdanoff 2014 ).
- Divergence of dry static energy: ERAI.DSEDIV (Trenberth et al. 2011 )
- Divergence of kinetic energy: ERAI.KEDIV
- Divergence of latent energy: ERAI.LEDIV
- Total energy tendency: ERAI.TETEN
- Latent energy tendency: ERAI.LETEN



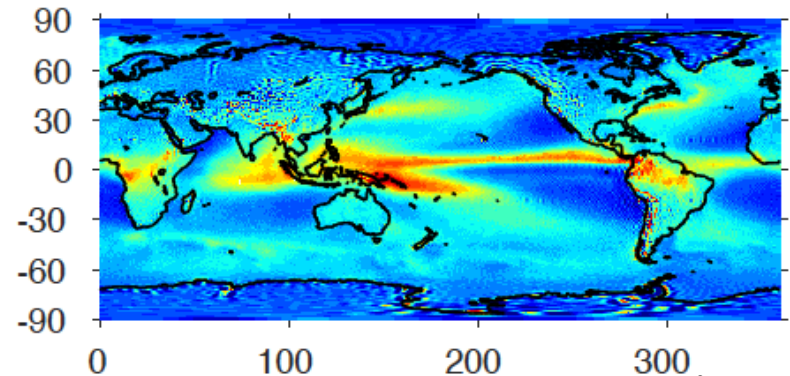
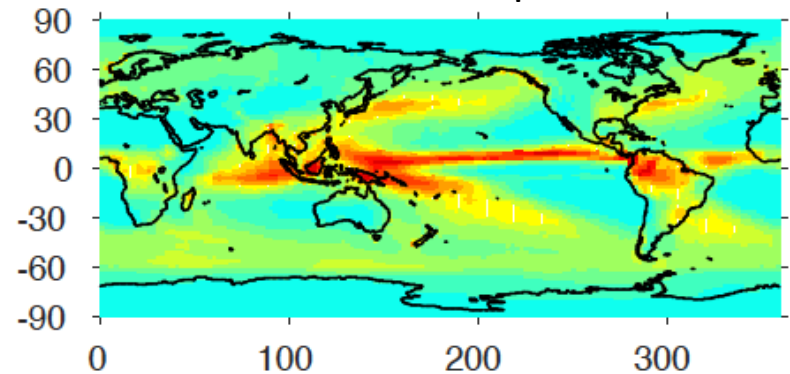
# Annual mean energy components on the same scale

Atm. net radiation

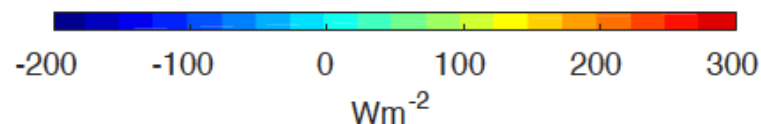


Sensible heat flux

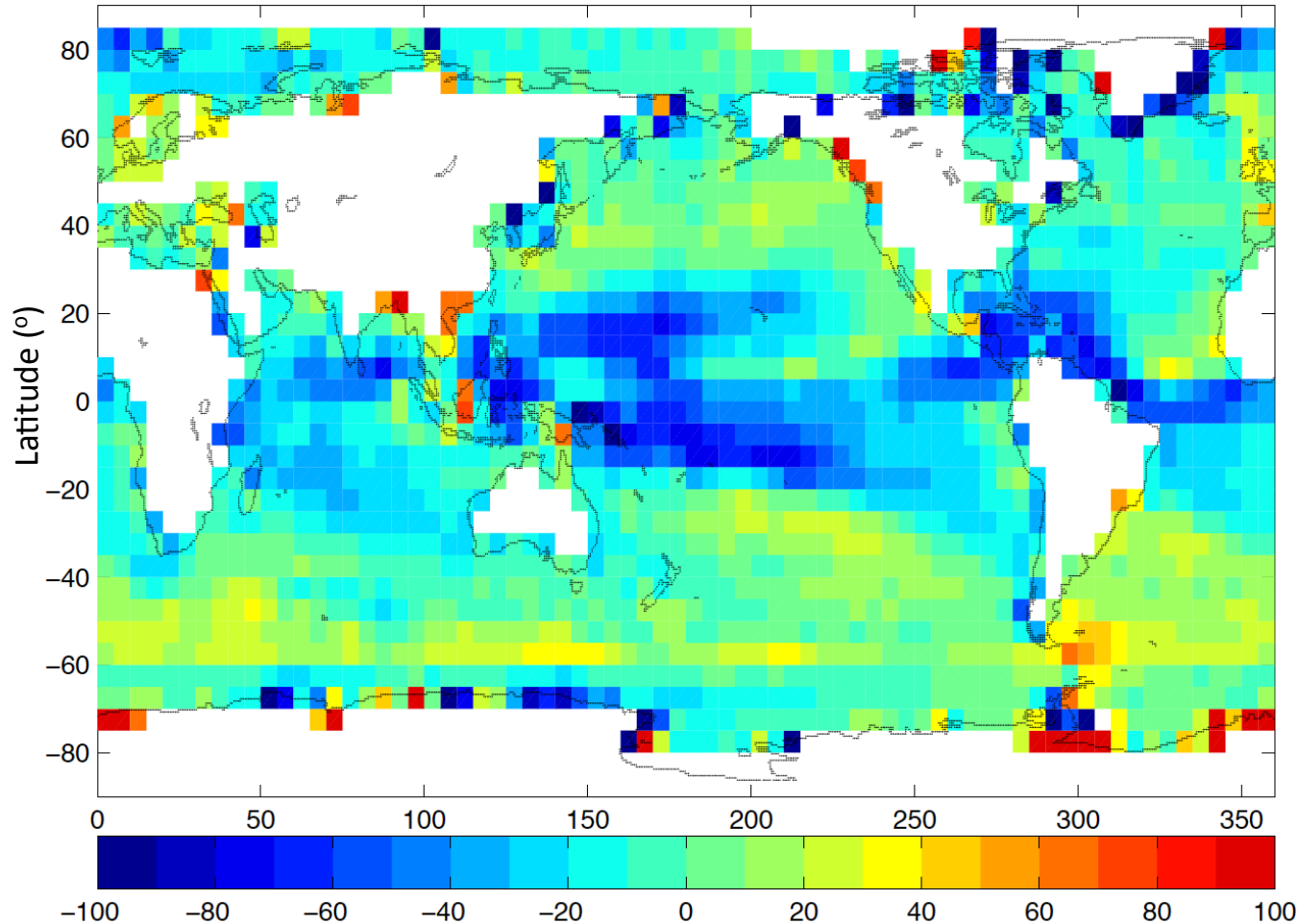
Precipitation rate



Dry static energy divergence



# Sum of all energy terms for the atmospheric column in $\text{Wm}^{-2}$ (10 year average)



## Negative area

- Precipitation is too small
- Divergence is too large
- Radiative cooling is too large

-Dry static and Kinetic energy tendency - divergence of dry static energy  
 -divergence of kinetic energy + atmospheric net irradiance + precipitation - surface sensible heat flux (positive downward)

$$-\frac{\partial(K_E + S_H + \Phi_s)}{\partial t} - \nabla_p \cdot (\mathbf{F}_K + \mathbf{F}_{DE}) + (R_T - R_s) + LP - H_s = 0$$

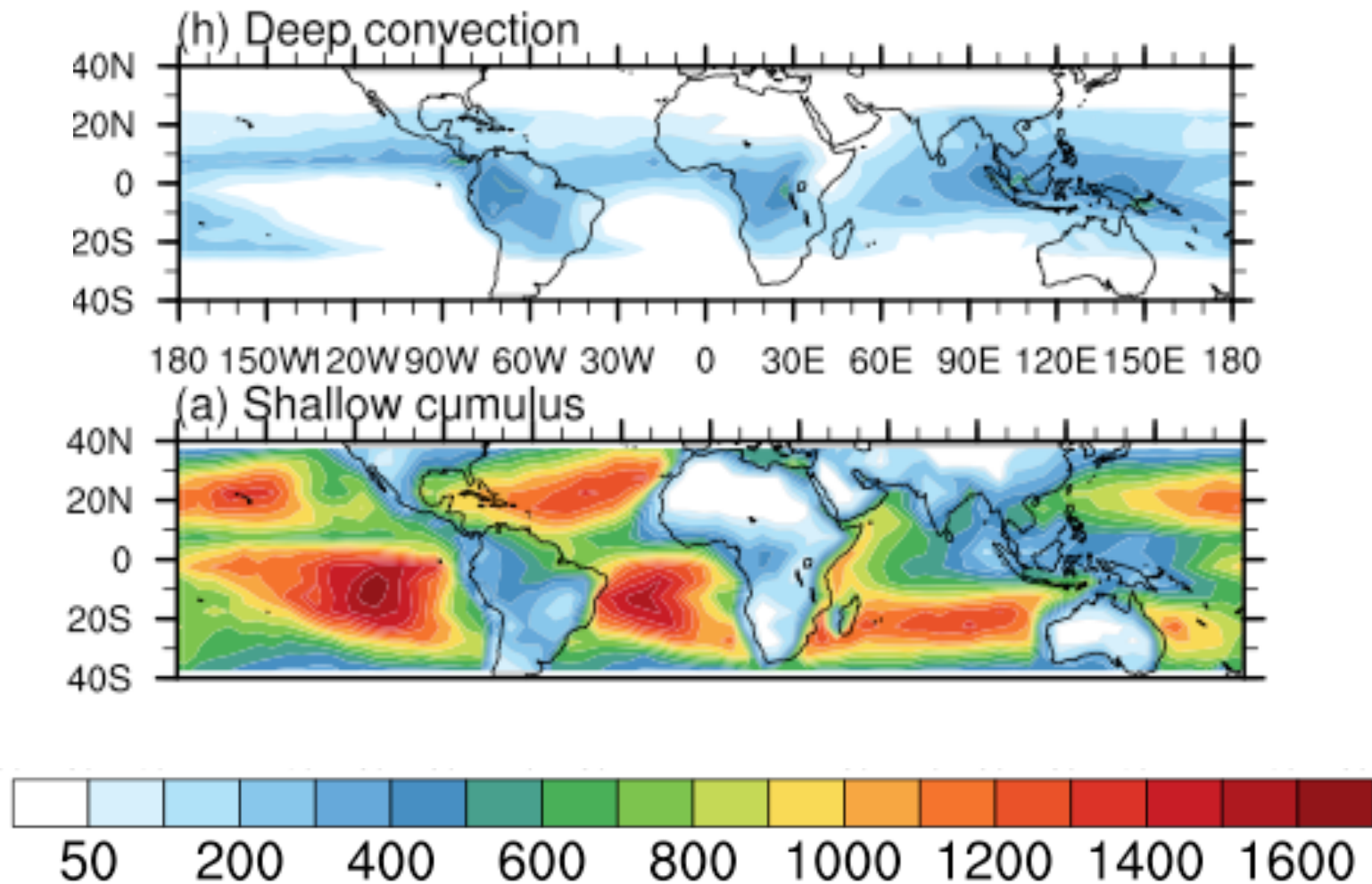
# Cloud object type definitions

**Table 2:** Cloud object type and selection criteria. Note that cloud objects are derived using only daytime data. Note also that 440 hPa and 680 hPa pressure levels are approximately 7 km and 3.4 km above the sea level in the tropics, respectively.

Cloud object type*	Cloud top height	Cloud optical depth	Cloud fraction	Current Latitude band
Tropical deep convection	< 440 (hPa)	> 10	1.0	25°S-25°N
Trade/shallow cumulus	> 680 hPa	—	0.1 – 0.4	40°N-40°S
Transition stratocumulus	> 680 hPa	—	0.4 – 0.99	40°N-40°S
Solid stratus	>680 hPa	—	0.99 – 1.0	40°N-40°S
Alto cumulus	440 hPa < h < 680 hPa	—	0.1 – 0.4	40°N-40°S
Transition alto cumulus	440 hPa < h < 680 hPa	—	0.4 – 0.99	40°N-40°S
Solid alto cumulus	440 hPa < h < 680 hPa	—	0.99 - 1.0	40°N-40°S
Cirrus	< 440hPa	< 10	0.1 – 0.4	40°N-40°S
Cirrocumulus	< 440 hPa	< 10	0.4 – 0.99	40°N-40°S
Cirrostratus	< 440 hPa	< 10	0.99 – 1.0	40°N-40°S

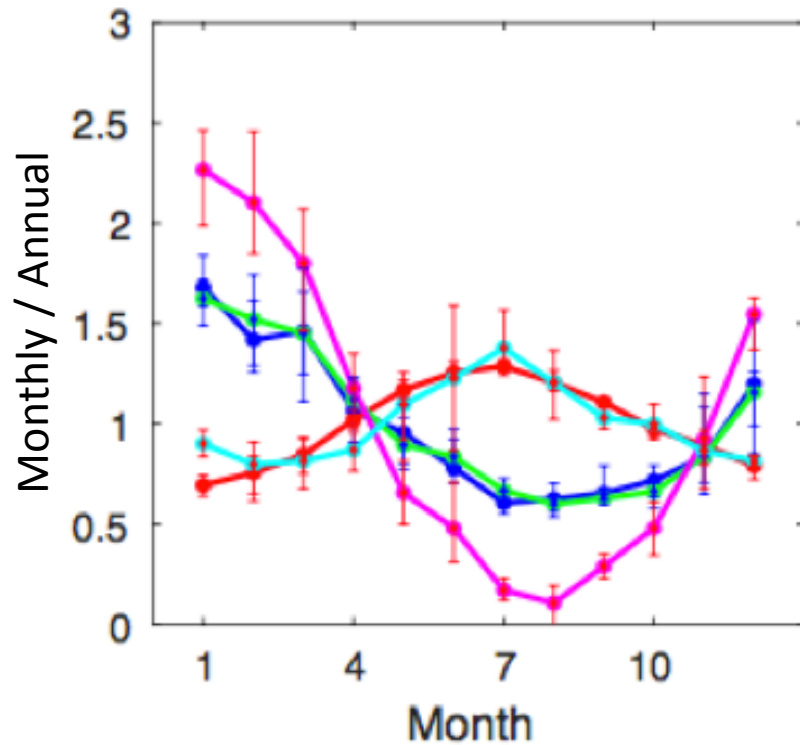
\* All cloud object types of given type are grouped into three size categories, 100 km to 150 km, 150 km to 300 km, and greater than 300 km.

# Spatial distribution of Number of cloud objects

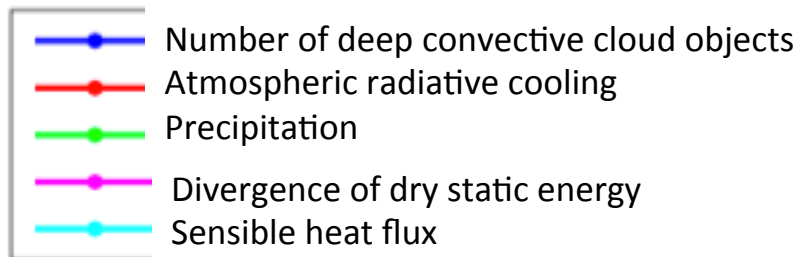
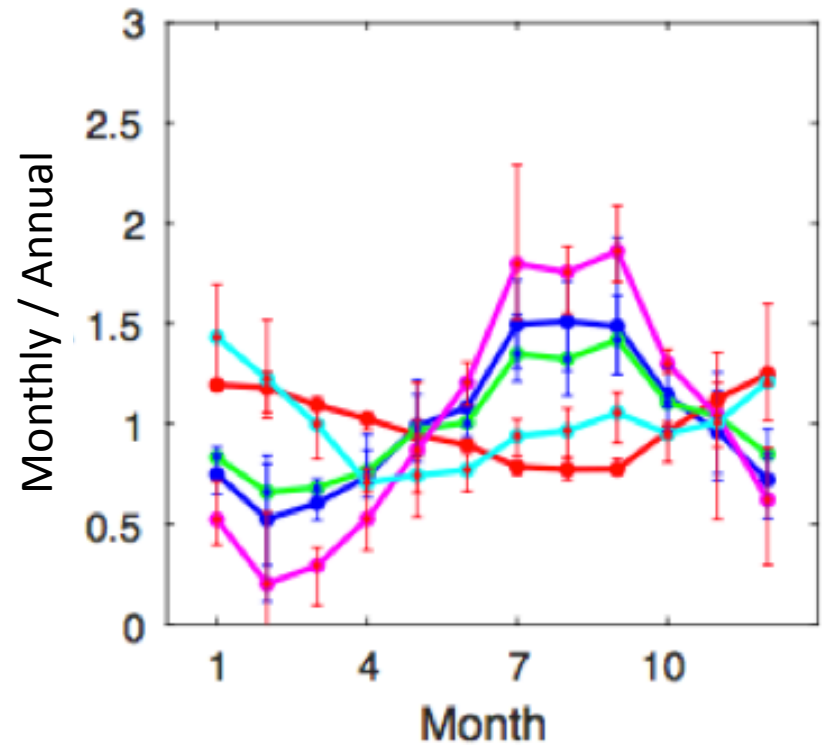


# Seasonal variability of energy flux components

Southern western Pacific ( $0^{\circ}$  to  $25^{\circ}\text{S}$ ;  $105^{\circ}\text{E}$  to  $180^{\circ}\text{E}$ )

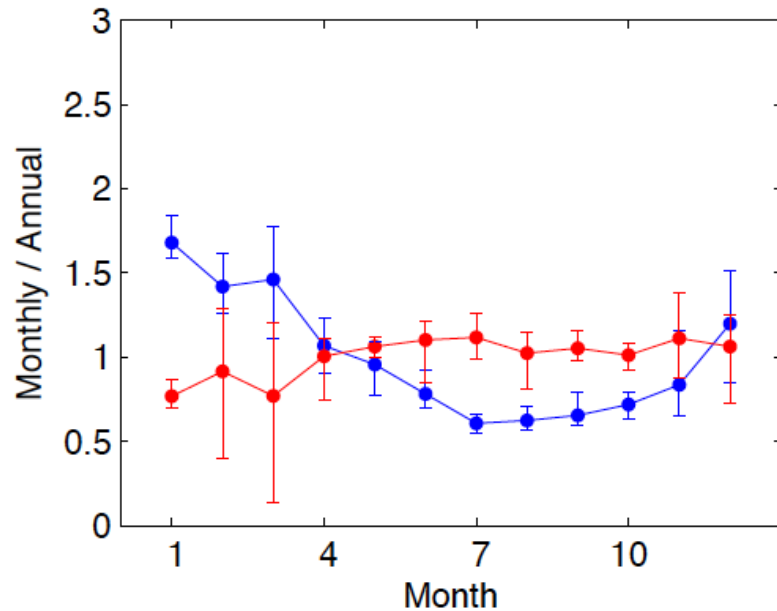


Northern western Pacific ( $0^{\circ}$  to  $25^{\circ}\text{N}$ ;  $105^{\circ}\text{E}$  to  $180^{\circ}\text{E}$ )

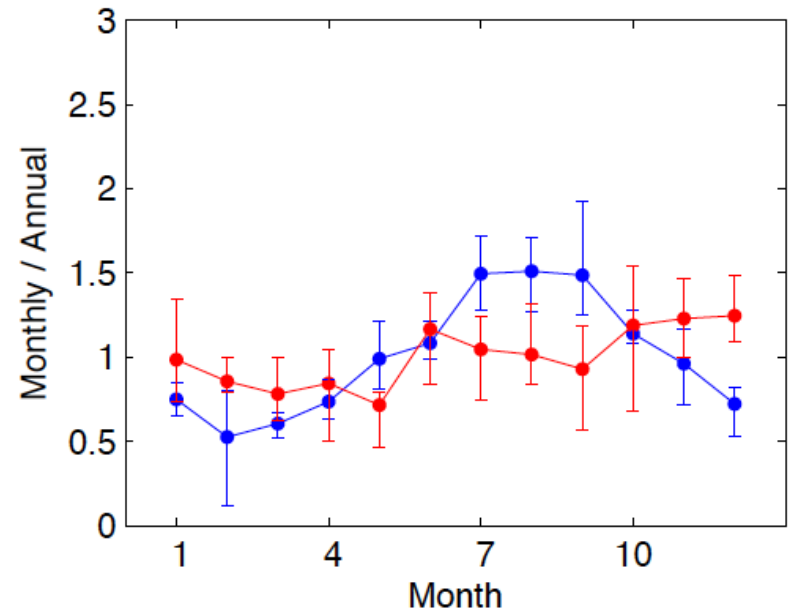


# Seasonal variability of atmospheric energy balance residual vs. deep convective clouds

Southern western Pacific ( $0^{\circ}$  to  $25^{\circ}\text{S}$ ;  $105^{\circ}\text{E}$  to  $180^{\circ}\text{E}$ )



Northern western Pacific ( $0^{\circ}$  to  $25^{\circ}\text{N}$ ;  $105^{\circ}\text{E}$  to  $180^{\circ}\text{E}$ )

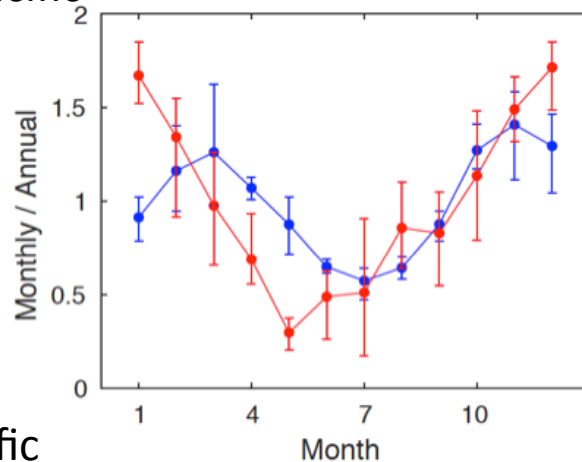


Blue: number of deep convective cloud objects

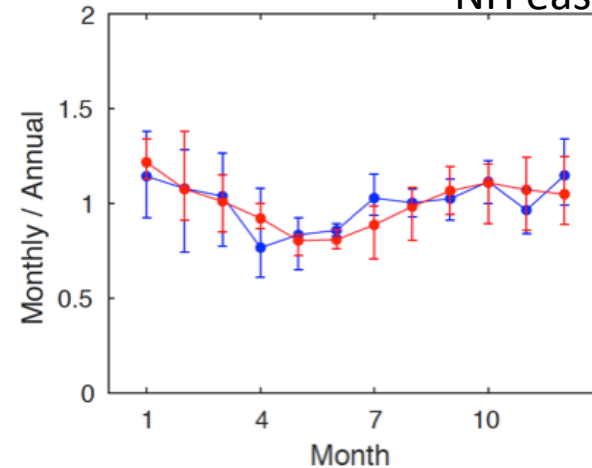
Red: Atmospheric energy balance residual + surface sensible heat flux

# Atmospheric energy balance residual vs. shallow cumulus clouds

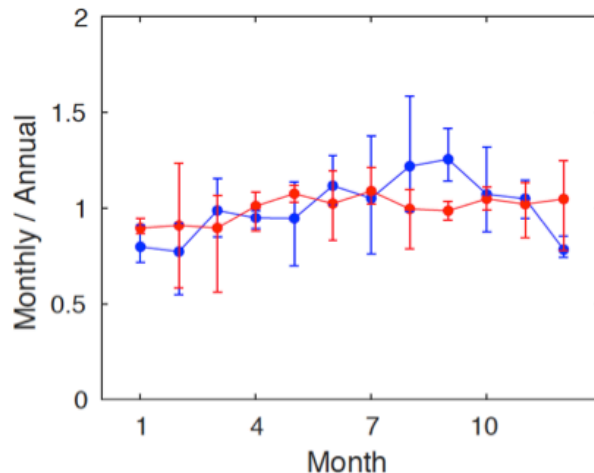
NH western Pacific



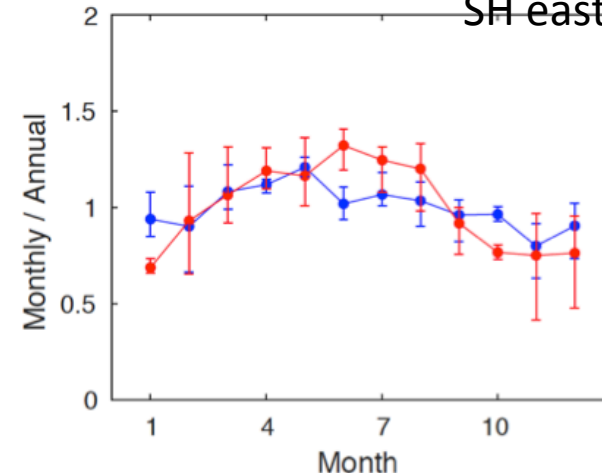
NH eastern pacific



SH western pacific



SH eastern pacific

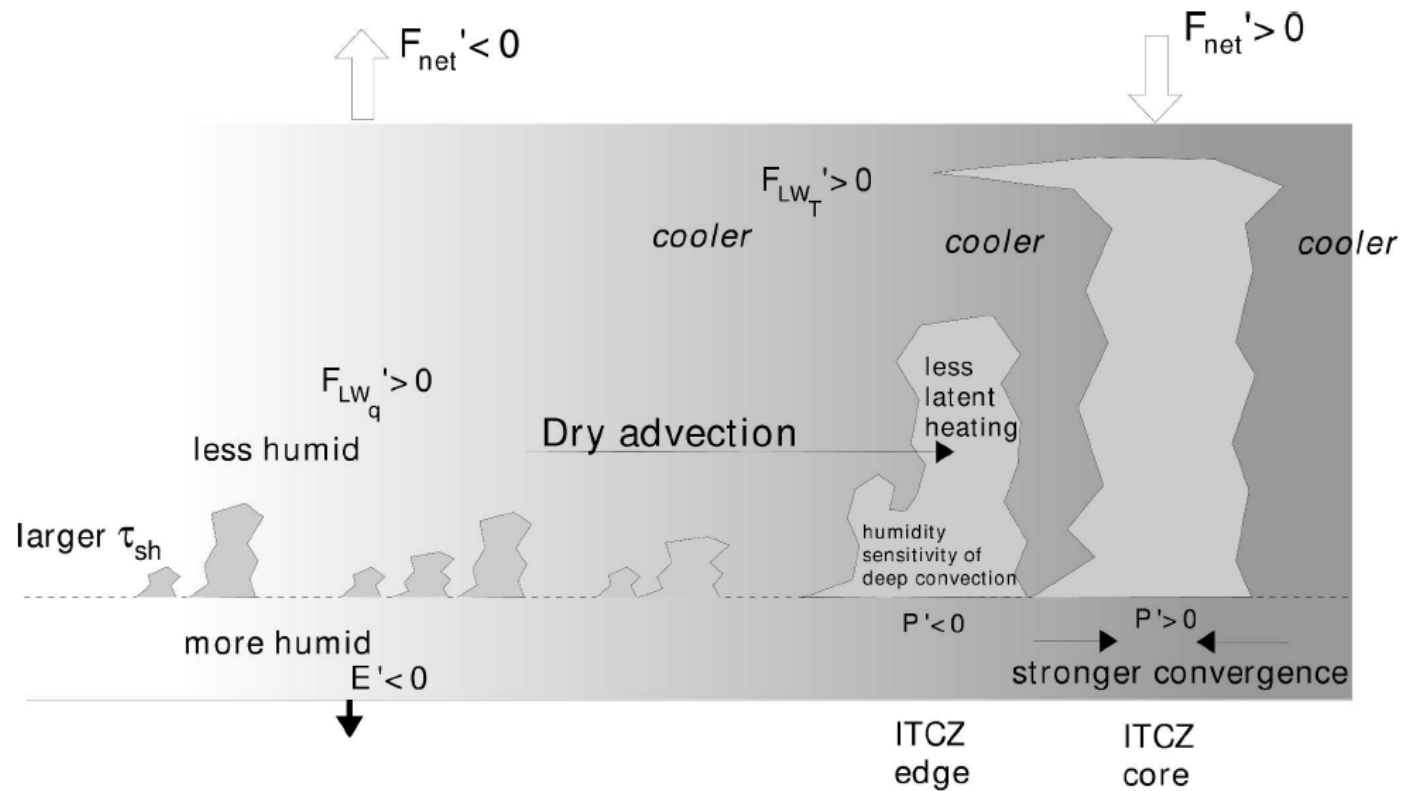


Blue: number of shallow cumulus cloud objects

Red: Atmospheric energy balance residual + surface sensible heat flux



# Proposed relationship between shallow cumulus and precipitation by deep convective clouds



More humid boundary layer  $\rightarrow$  more shallow cumulus  $\rightarrow$  area decrease  $\leftarrow$   
 $\rightarrow$  dryer free troposphere  $\rightarrow$  narrower ITCZ  
 $\rightarrow$  stronger precipitation by deep convective clouds



# Possible cause

- A study by Berg et al. (2010) shows that the precipitation rate over tropical eastern Pacific estimated from the CloudSat radar that is not included in the estimate from the TRMM radar is about 0.4 to 0.5 mm day<sup>-1</sup>, which is  $\sim 13 \text{ Wm}^{-2}$ , although the 150 km radius range over Barbuda area-averaged precipitation rate by shallow cumuli estimated by Nuijens et al. (2009) reaches about  $35 \text{ Wm}^{-2}$ .
- Kato (2009) shows that the atmospheric cooling by clouds with the top height pressure greater than 665 hPa is 0 to  $-25 \text{ Wm}^{-2}$  over tropics. According to Oreopoulos et al. (2014) low-level clouds account for roughly 50% of clouds present in cloud regime 2. These lead to about a  $10 \text{ Wm}^{-2}$  contribution to atmospheric cooling by shallow cumulus clouds.
- Enhanced intense precipitations within deep convective clouds are missed by satellite observations
- It is also possible that cumulus congestus are sometimes present under cirrostratus.

# Summary and conclusions

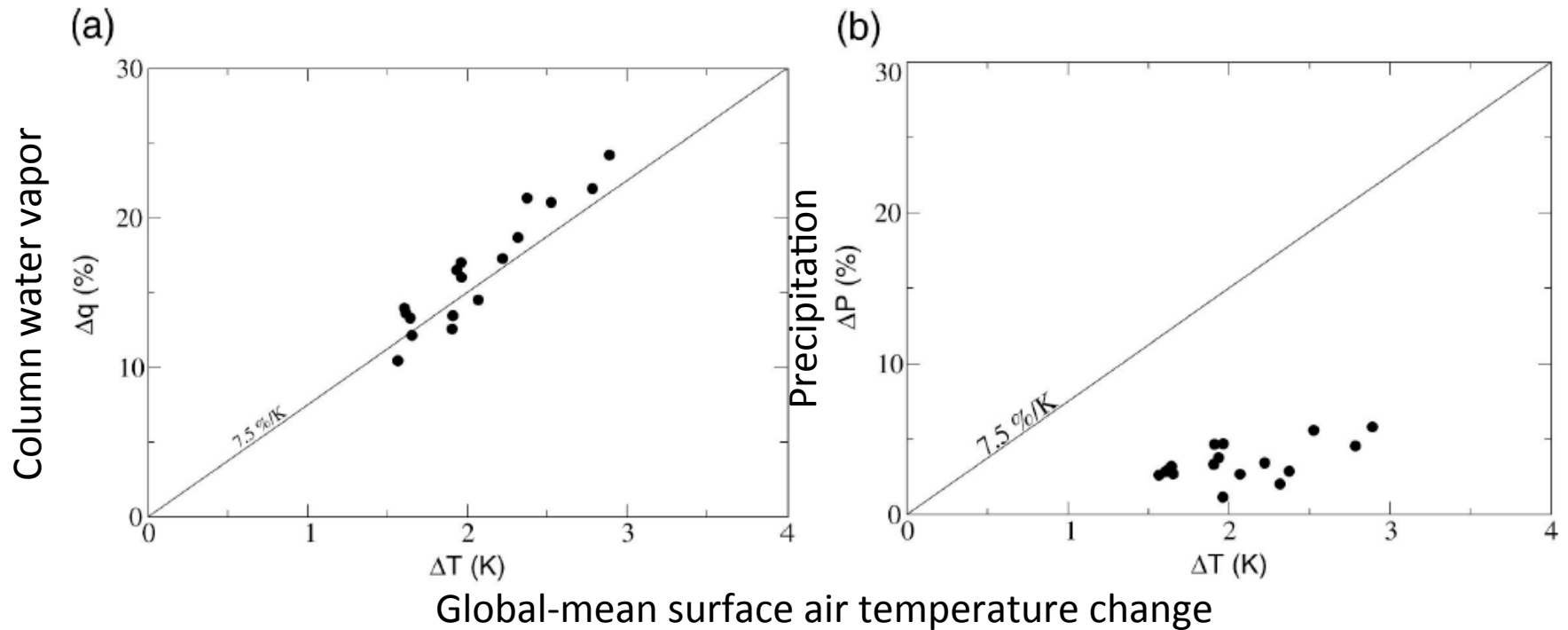
- Current status: global surface energy imbalance 10 to 15  $\text{Wm}^{-2}$ 
  - Need to understand permissible energy imbalance derived from observations (tolerance)
- Regional atmospheric column energy imbalance exists over tropical ocean
  - Energy imbalance can be related to cloud types or weather states
  - Radiative net flux, precipitation, and dry static energy divergence are three large terms contributing atmospheric energy balance in a column.
  - Values and even the sign of imbalance vary spatially and temporally
  - Regions with large negatives over western pacific tend to coincide with areas with large deep convective cloud objects (> 300 km) and shallow convective clouds occupy a large area (> 300 km).

# Back ups

# Why (balancing) energy budget is important

- Non-uniform energy distribution received from the sun over the globe is the driver of dynamics and hydrological cycle
- Radiative forcing alters the radiative component
- All forms (components), radiation, precipitation, atmospheric dynamics, and surface fluxes are related by the conservation of energy and not independent so that a change in one term affects other terms (i.e. all need to be consistent)
- Satellite observations of precipitation, radiation, surface turbulent fluxes, and ocean temperature (heating rate) can complement each other

# Column water vapor, precipitation and radiation change



Held and Soden (2006, J Climate)

AR4 models suggest that water vapor in the atmosphere increases at the rate of  $\sim 7.5\% \text{ K}^{-1}$ , obeying Clausius-Clapeyron relationship. But precipitation increases at a slower rate, driven by surface net irradiance change (e.g. Stephens and Ellis 2008).

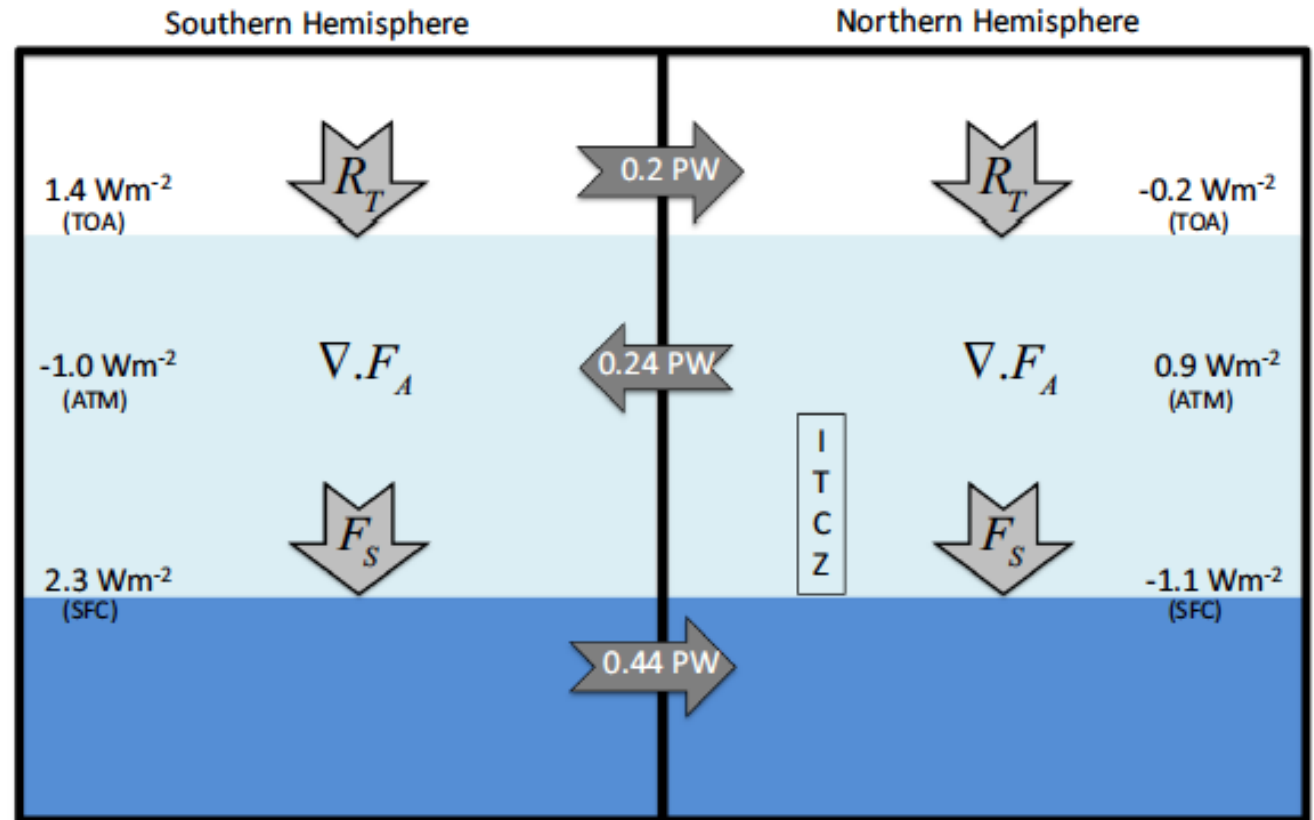
# Energy transport, precipitation, radiation, and surface flux

Hemispherical asymmetry of energy flux into the atmosphere and ocean

Energy transport by dynamics

Location of Hadley circulation

Hemispherical precipitation asymmetry



# Estimated surface irradiance uncertainty

TABLE 5. Summary of uncertainties in the irradiance computed with satellite-derived cloud and aerosol properties in  $\text{W m}^{-2}$  (after Kato et al. 2012).

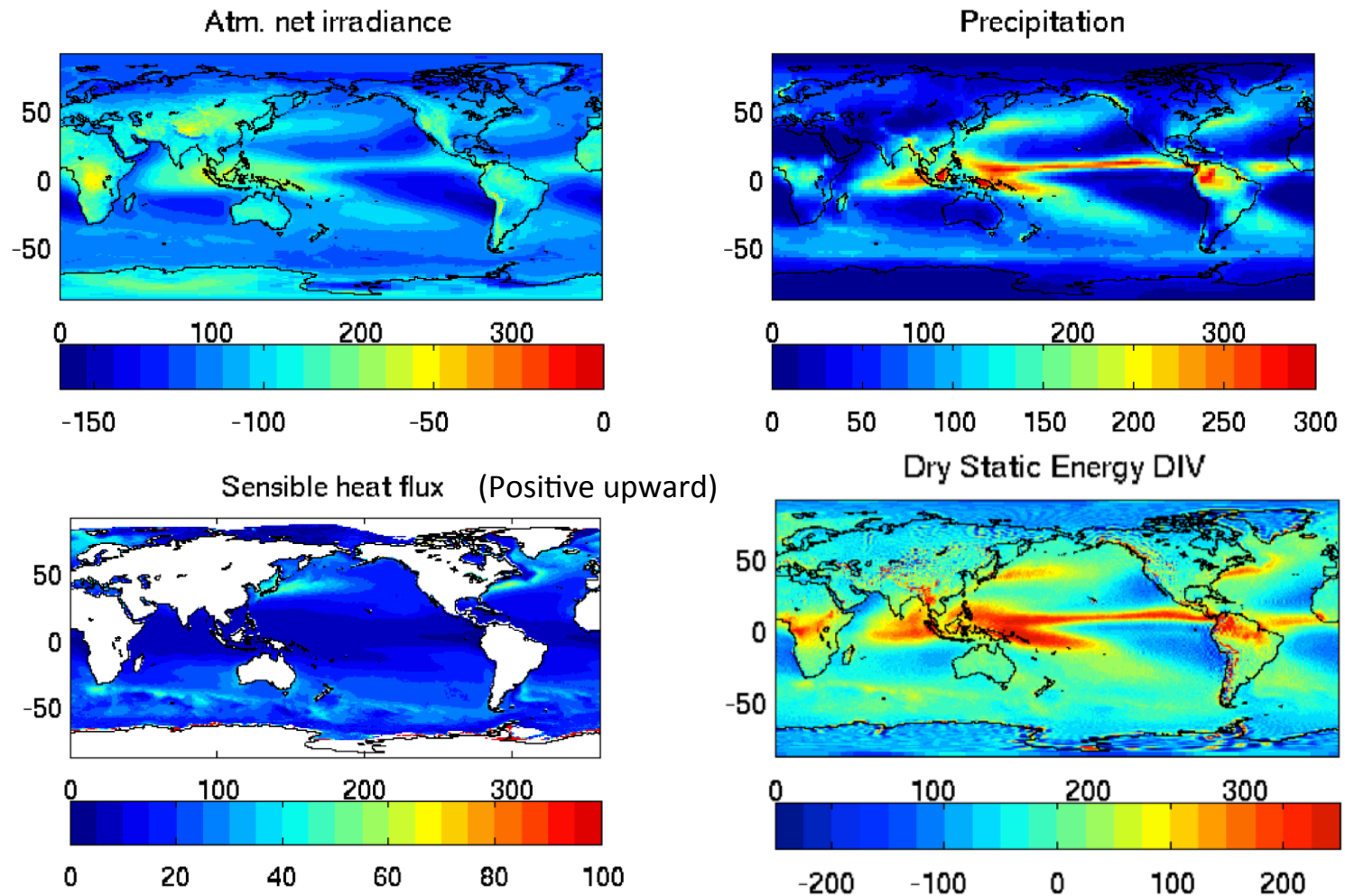
		Mean value	Estimated uncertainty			
			Monthly gridded	Monthly zonal	Monthly global	Annual global
Downward longwave	Ocean+land	345	14	11	7	7
	Ocean	354	12	10	7	7
	Land	329	17	15	8	7
Upward longwave	Ocean+land	398	15	8	3	3
	Ocean	402	13	9	5	5
	Land	394	19	15	5	4
Downward shortwave	Ocean+land	192	10	8	6	4
	Ocean	190	9	8	5	4
	Land	203	12	10	7	5
Upward shortwave	Ocean+land	23	11	3	3	3
	Ocean	12	11	3	3	3
	Land	53	12	8	6	6

Kato et al. J Climate 2013

Monthly mean RMS difference between computed and observed irradiance (nearly equivalent to the monthly gridded uncertainty)

	Ocean	Land
LW down RMS	6	11
SW down RMS	11	13

# Annual mean 1deg by 1deg Atmospheric net irradiance, precipitation, and surface sensible heat flux

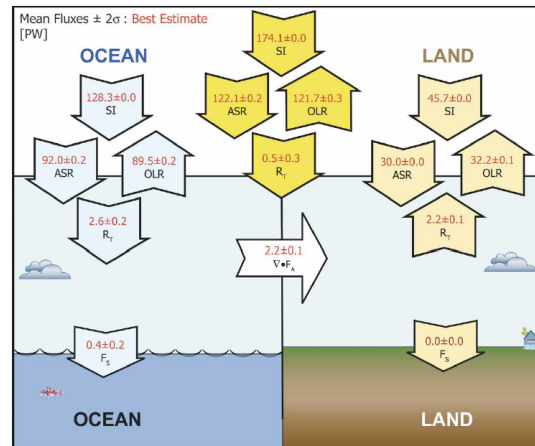


Three large terms are Atmospheric net irradiance, precipitation, and dry static energy divergence



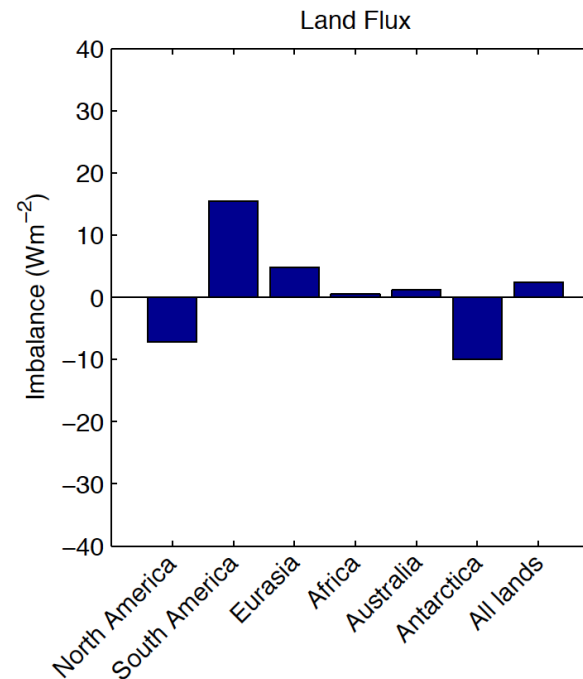
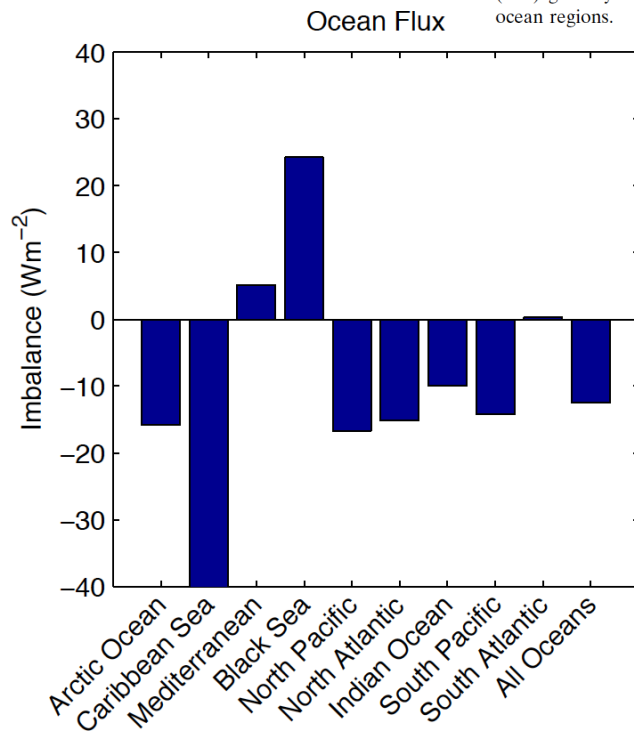
# Regional imbalance (Flux)

Precip.+Rad.-DSEDIV-KEDIV-TETEN+LETEN+SH



Fasulo and Trenberth (2008 J. Climate)

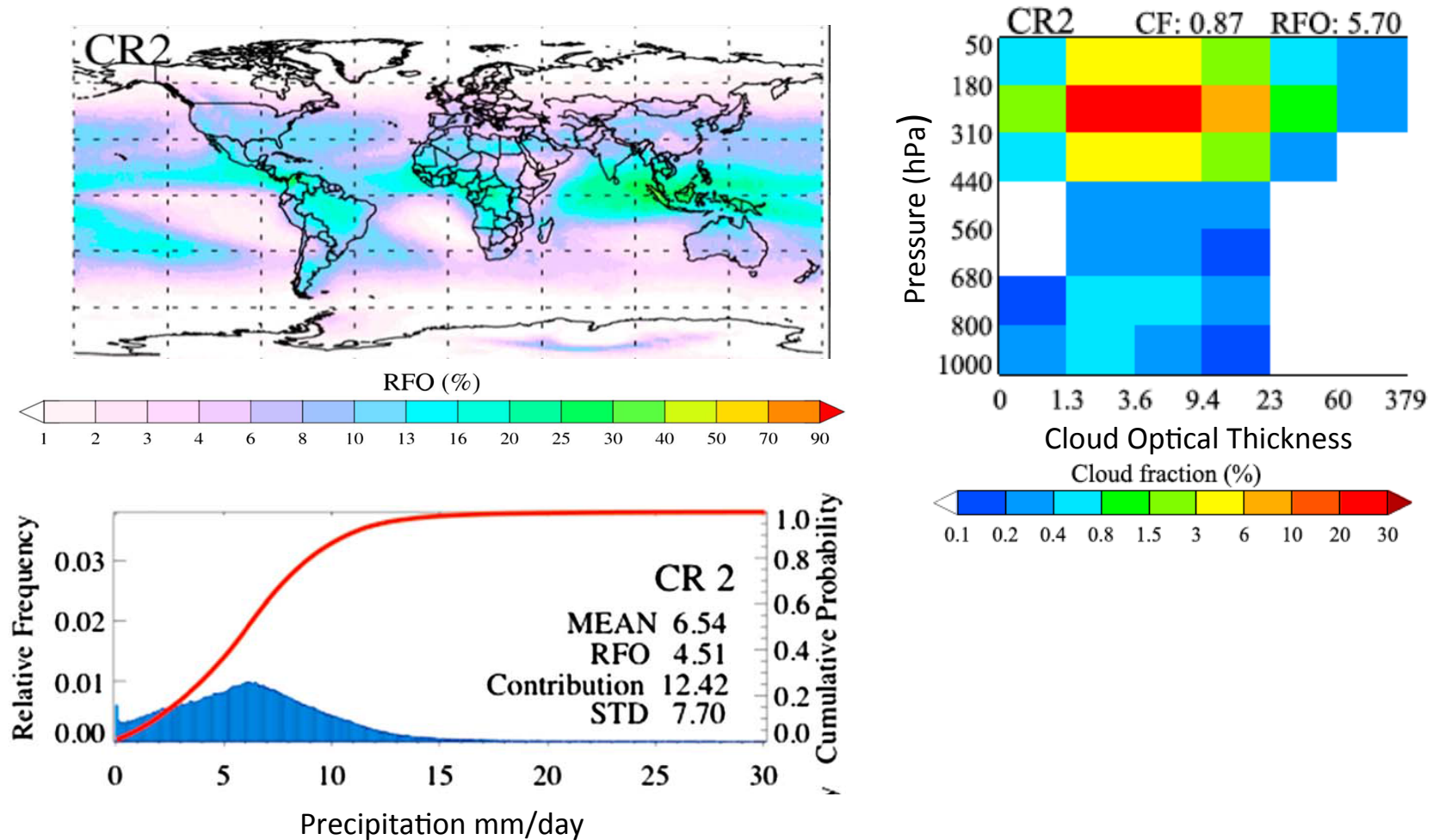
FIG. 2. CERES-period-mean best-estimate FM1 TOA fluxes (PW) globally and for the (right) global land and (left) global ocean regions.



Consistent with L'Ecuyer et al. 2015 who compute surface energy balance

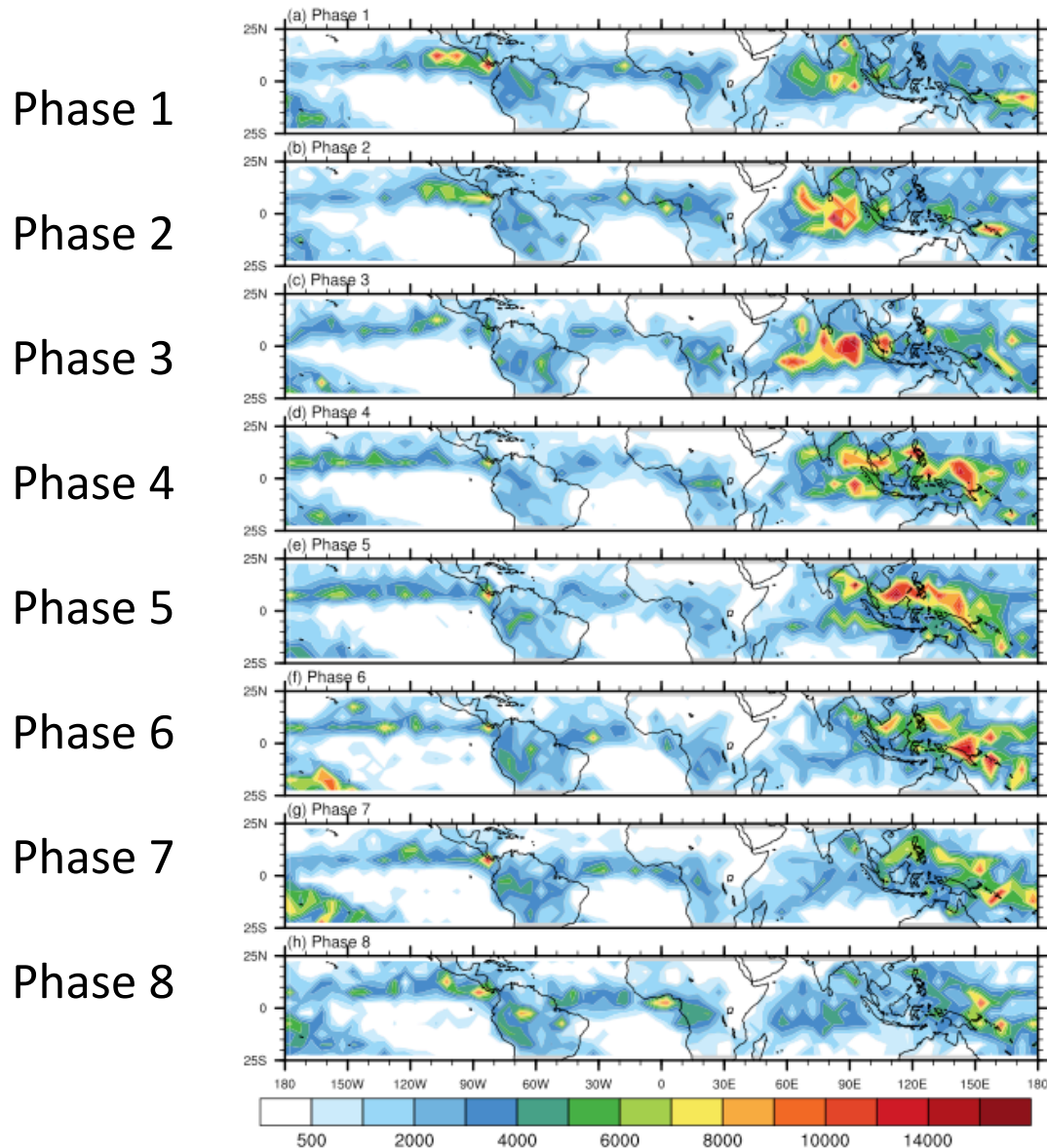
Land sensible heat fluxes are taken from L'Ecuyer et al. 2015 (J. Climate)

# Regional energy imbalance vs. cloud profile, type and cloud regime (or weather state)

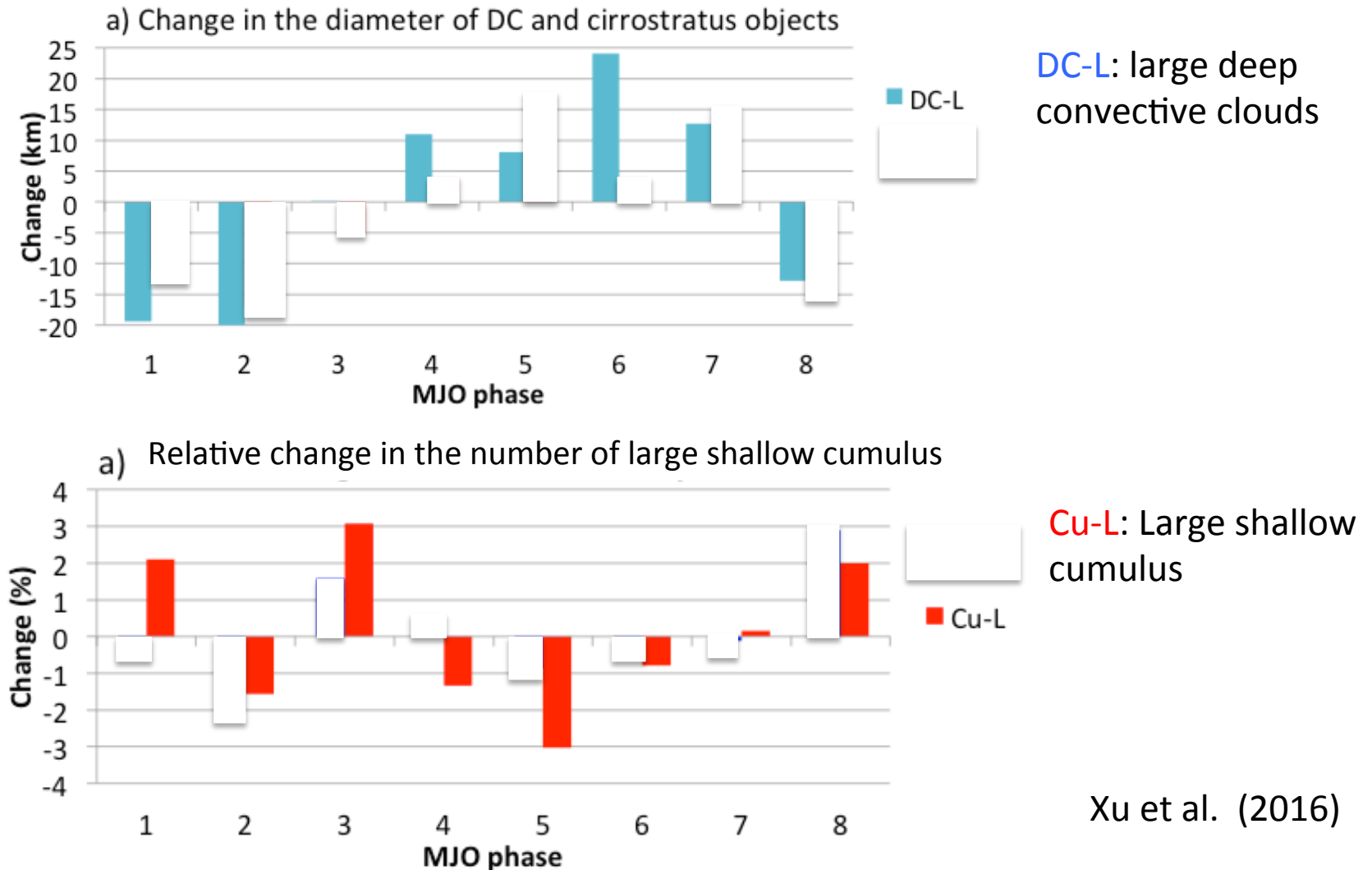


Oreopoulos et al. (2014)

Horizontal distributions of the total number of satellite footprints of deep convective cloud objects in  $5^\circ \times 5^\circ$  grids as a function of MJO phases (Phases 1 to 8 from the top to the bottom).



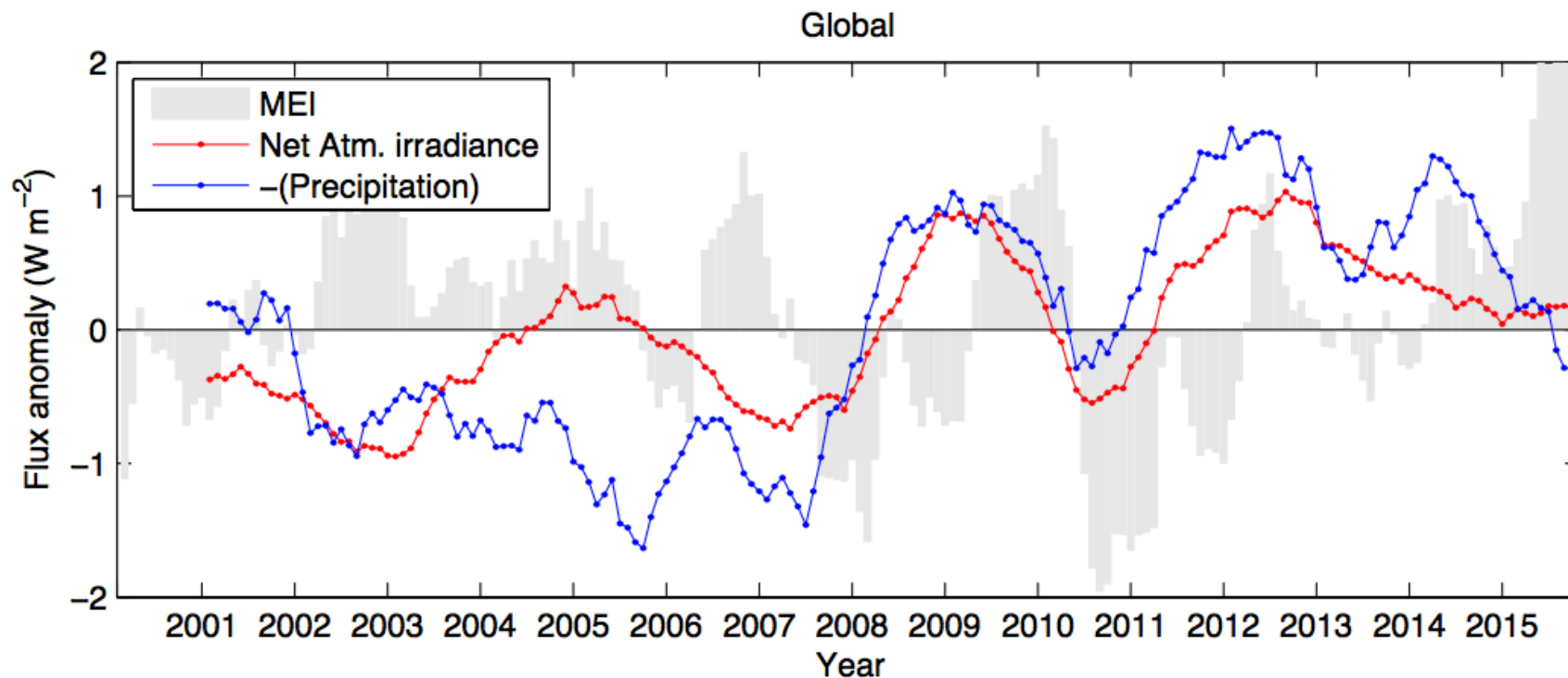
# Number of shallow cumulus cloud objects vs. deep convective cloud object size



# Atmospheric irradiance divergence vs. precipitation anomalies

Radiation is probably not responsible for the  $15 \text{ Wm}^{-2}$  surface energy balance residual, but the error in anomalies is less certain.

Current accuracy level is  $\sim 0.8 \text{ Wm}^{-2}$  per decade (at a 60% confidence level) for both surface downward LW and SW irradiances (CERES white paper) while precipitation changes at the rate of  $\sim 0.3 \text{ Wm}^{-2}$  per decade ( $2\% \text{ K}^{-1}$ )



With 12 month running mean

Surface sensible heat anomalies are missing